International Standard

ISO 25178-604

Geometrical product specifications (GPS) — Surface texture: Areal —

Part 604: Design and characteristics of non-contact (coherence scanning interferometry) instruments

Spécification géométrique des produits (GPS) — État de surface: Surfacique —

Partie 604: Conception et caractéristiques des instruments sans contact (à interférométrie par balayage à cohérence)

Second edition
2025-02

Reference number
ISO 25178-604:2025(en)

ISO copyright office
CP 401 • Ch. de Blandonnet 8
CH-1214 Vernier, Geneva
Phone: +41 22 749 01 11
Email: copyright@iso.org
Website: www.iso.org

Published in Switzerland

Contents

Page

Foreword

ISO (the International Organization for Standardization) is a worldwide federation of national standards bodies (ISO member bodies). The work of preparing International Standards is normally carried out through ISO technical committees. Each member body interested in a subject for which a technical committee has been established has the right to be represented on that committee. International organizations, governmental and non-governmental, in liaison with ISO, also take part in the work. ISO collaborates closely with the International Electrotechnical Commission (IEC) on all matters of electrotechnical standardization.

The procedures used to develop this document and those intended for its further maintenance are described in the ISO/IEC Directives, Part 1. In particular, the different approval criteria needed for the different types of ISO document should be noted. This document was drafted in accordance with the editorial rules of the ISO/IEC Directives, Part 2 (see www.iso.org/directives).

ISO draws attention to the possibility that the implementation of this document may involve the use of (a) patent(s). ISO takes no position concerning the evidence, validity or applicability of any claimed patent rights in respect thereof. As of the date of publication of this document, ISO had not received notice of (a) patent(s) which may be required to implement this document. However, implementers are cautioned that this may not represent the latest information, which may be obtained from the patent database available at www.iso.org/patents. ISO shall not be held responsible for identifying any or all such patent rights.

Any trade name used in this document is information given for the convenience of users and does not constitute an endorsement.

For an explanation of the voluntary nature of standards, the meaning of ISO specific terms and expressions related to conformity assessment, as well as information about ISO's adherence to the World Trade Organization (WTO) principles in the Technical Barriers to Trade (TBT), see www.iso.org/iso/foreword.html.

This document was prepared by Technical Committee ISO/TC 213, *Dimensional and geometrical product specifications and verification*, in collaboration with the European Committee for Standardization (CEN) Technical Committee CEN/TC 290, *Dimensional and geometrical product specification and verification,* in accordance with the Agreement on technical cooperation between ISO and CEN (Vienna Agreement).

This second edition cancels and replaces the first edition (ISO 25178-604:2013), which has been technically revised.

The main changes are as follows:

— removal of the terms and definitions now specified in ISO 25178-600;

— revision of all terms and definitions for clarity and consistency with other ISO standards documents;

— addition of Clause 4 for instrument requirements, which summarizes normative features and characteristics;

— addition of Clause 5 on metrological characteristics;

— addition of Clause 6 on design features, which clarifies types of instruments relevant to this document;

— addition of an information flow concept diagram in Clause 4;

— revision of Annex A describing the principles of instruments addressed by this document;

— addition of Annex B on metrological characteristics and influence quantities; replacement of the normative table of influence quantities with an informative description of common error sources and how these relate the metrological characteristics in ISO 25178-600.

A list of all parts in the ISO 25178 series can be found on the ISO website.

Any feedback or questions on this document should be directed to the user’s national standards body. A complete listing of these bodies can be found at www.iso.org/members.html

Introduction

This document is a geometrical product specification (GPS) standard and is to be regarded as a general GPS standard (see ISO 14638). It influences chain link F of the chains of standards on profile and areal surface texture.

The ISO GPS matrix model given in ISO 14638 gives an overview of the ISO GPS system of which this document is a part. The fundamental rules of ISO GPS given in ISO 8015 apply to this document and the default decision rules given in ISO 14253-1 apply to the specifications made in accordance with this document, unless otherwise indicated.

For more detailed information on the relation of this document to other standards and the GPS matrix model, see Annex C.

This document includes terms and definitions relevant to the coherence scanning interferometry (CSI) instrument for the measurement of areal surface topography. Annex A briefly summarizes CSI instruments and methods to clarify the definitions and to provide a foundation for Annex B, which describes common sources of uncertainty and their relation to the metrological characteristics of CSI.

NOTE Portions of this document, particularly the informative sections, describe patented systems and methods. This information is provided only to assist users in understanding the operating principles of CSI instruments. This document is not intended to establish priority for any intellectual property, nor does it imply a license to proprietary technologies described herein.

Geometrical product specifications (GPS) — Surface texture: Areal —

Part 604:
Design and characteristics of non-contact (coherence scanning interferometry) instruments

1 Scope

This document specifies the design and metrological characteristics of coherence scanning interferometry (CSI) instruments for the areal measurement of surface topography. Because surface profiles can be extracted from surface topography data, the methods described in this document are also applicable to profiling measurements.

2 Normative references

The following documents are referred to in the text in such a way that some or all of their content constitutes requirements of this document. For dated references, only the edition cited applies. For undated references, the latest edition of the referenced document (including any amendments) applies.

ISO 25178-600:2019, *Geometrical product specifications (GPS) — Surface texture: Areal — Part 600: Metrological characteristics for areal topography measuring methods*

3 Terms and definitions

For the purposes of this document, the terms and definitions given in ISO 25178-600 and the following apply.

ISO and IEC maintain terminology databases for use in standardization at the following addresses:

— ISO Online browsing platform: available at https://www.iso.org/obp

— IEC Electropedia: available at https://www.electropedia.org/

3.1
coherence scanning interferometry
CSI
surface topography measurement method wherein the localization of *interference fringes* (3.7) during a scan of optical path length provides a means to determine a surface topography map

Note 1 to entry: The optical path length difference is the difference in optical path length, including the effect of geometry and refractive index, between the measurement and reference paths of an interferometer (see ISO 10934:2020, 3.3.1).

Note 2 to entry: CSI uses a broad illumination spectral bandwidth or the illumination geometry, or both, to localize the interference fringes.

Note 3 to entry: CSI uses either fringe localization alone or in combination with *interference phase* (3.8) evaluation, depending on the surface type, desired surface topography repeatability and software capabilities.

Note 4 to entry: Table 1 provides a list of alternative terms for CSI that are within the scope of this document.

Table 1 — Summary of common alternative terms for CSI

Term	Bibliography
Coherence probe microscopy Coherence radar Coherence correlation interferometry	References [13], [14], [15], [16], [17] and [18]
White light interferometry White light scanning interferometry Scanning white light interferometry	References [19], [20] and [21]
Vertical scanning interferometry Height scanning interferometry	References [22] and [23]
Full-field optical coherence tomography	Reference [24]

[SOURCE: ISO 25178-6:2010, 3.3.5, modified — Note 1 to entry has been replaced by Notes 1 to 4 to entry.]

3.2
coherence scanning interferometry scan
CSI scan
mechanical or optical scan which varies the optical length of either the reference path or measurement path to vary the optical path difference

Note 1 to entry: The imaging optics is nominally parallel to the axial scan axis of the microscope (see ISO 25178-607:2019, 3.5).

Note 2 to entry: A *CSI signal* (3.3) can correspond to a sequence of electronic camera detections of intensity values during a CSI scan (see Annex A).

Note 3 to entry: In CSI, the most common (but not exclusive) scanning means is a physical adjustment of the path length of an interferometer (see ISO/TR 14999-2).

Note 4 to entry: Mechanical means for performing the CSI scan can be motorized or piezo-electrically driven stages or others, depending on the instrument design, the linearity and consistency of the CSI scan, or the desired maximum *CSI scan length* (3.5).

3.3
coherence scanning interferometry signal
CSI signal
correlogram
white light interferometry signal
intensity data recorded for an individual image point or camera pixel as a function of *CSI scan* (3.2) position

Note 1 to entry: See Figure 1 for a simulated example CSI signal for an *equivalent wavelength* (3.12) of 450 nm and a measurement optical bandwidth of 110 nm at full width half maximum (see ISO 25178-600:2019, 3.3.2) and a low illumination numerical aperture (see ISO 10934:2020, 3.1.10.4 and ISO 25178-600:2019, 3.3.6).

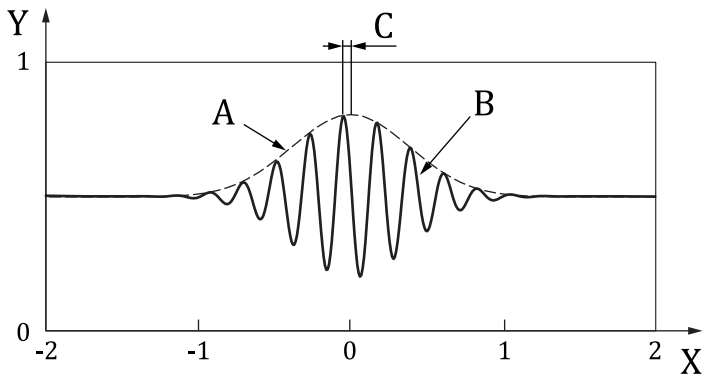

Key

X	CSI scan position expressed in micrometres	B	interference fringes
Y	intensity	C	phase gap
A	modulation envelope (calculated)		

Figure 1 — Defined features of a CSI signal

3.4
coherence scanning interferometry scan increment
CSI scan increment
distance travelled by the *CSI scan* (3.2) between data captures

Note 1 to entry: A data capture can be a single image point or a camera frame.

Note 2 to entry: The CSI scan increment is most often small enough to sample each *interference fringe* (3.7) at several points, e.g. four camera frames per fringe, consistent with the Nyquist criterion. Sub-Nyquist sampling is also possible for higher data acquisition speeds, at the cost of higher measurement noise.

3.5
coherence scanning interferometry scan length
CSI scan length
total range of physical path length traversed by the *CSI scan* (3.2)

Note 1 to entry: The CSI scan length should normally be sufficiently long so as to capture the desired surface topography range plus at least a portion of the modulation envelope width.

3.6
coherence scanning interferometry scanning rate
CSI scanning rate
CSI scan speed
speed at which the *CSI scan* (3.2) is executed

Note 1 to entry: For a linear CSI scan, the CSI scanning rate is the camera frame rate multiplied by the *CSI scan increment* (3.4).

3.7
interference fringe
<coherence scanning interferometry> modulating portion of the *CSI signal* (3.3), related to the interference effect and generated by the variation of optical path length during the *CSI scan* (3.2)

Note 1 to entry: The interference fringes are approximately sinusoidal as a function of scan position.

Note 2 to entry: See Figure 1 for an illustration of the interference fringes of a CSI signal.

Note 3 to entry: The term “interferogram” is often used to describe the image of an interference fringe pattern recorded by a single camera frame (see ISO/TR 14999-2:2019, 6.2). An interference fringe in an interferogram is an attribute of the interference pattern; whereas an interference fringe in *CSI* (3.1) refers to an attribute of a scan-dependent signal, as illustrated in Figure 1.

3.8
interference phase
<coherence scanning interferometry> phase corresponding to the sinusoidal form of the *interference fringes* (3.7) in the *CSI signal* (3.3)

3.9
modulation amplitude
interference fringe visibility
interference fringe contrast
<coherence scanning interferometry> one-half the peak-to-valley variation or equivalent measure of the amplitude of the *interference fringes* (3.7)

Note 1 to entry: See ISO/TR 14999-2:2019, 4.1.2 and 5.2.5, for example uses of the terms “visibility” and “contrast” as synonyms, respectively.

Note 2 to entry: The modulation amplitude of a *CSI signal* (3.3) varies as a function of scan position.

3.10
modulation envelope
fringe contrast envelope
fringe visibility function
fringe visibility envelope
degree of coherence as a function of CSI scan position
overall variation in the *modulation amplitude* (3.9) of a *CSI signal* (3.3) as a function of scan position

Note 1 to entry: See Figure 1 for an illustration of the modulation envelope of a *CSI signal* (3.3).

Note 2 to entry: The modulation envelope is a consequence of limited optical coherence, which follows from using a spectrally broadband light source (white light) or a spatially extended light source, or both.

Note 3 to entry: The modulation envelope is calculated as a function of scan position that depends on the data analysis method.

3.11
coherence scanning interferometry signal processing option
CSI signal processing option
processing selection that determines whether the software makes use of the *modulation envelope* (3.10), the *interference phase* (3.8), a model-based analysis or other approach to interpreting the *CSI signal* (3.3)

Note 1 to entry: See Clause A.3.

3.12
equivalent wavelength
λ_{eq}
<coherence scanning interferometry> change in surface topography height which corresponds to the scan length between two successive *interference fringes* (3.7) in the *CSI signal* (3.3) near the maximum value of the *modulation envelope* (3.10) of a CSI signal

Note 1 to entry: The equivalent wavelength is a definition in the context of CSI for the measurement optical wavelength, defined in ISO 25178-600:2019, 3.3.3, as the “effective value of the wavelength of the light used to measure a surface”.

Note 2 to entry: The measurement optical wavelength is affected by conditions such as the light source spectrum, spectral transmission of the optical components and spectral response of the image sensor array.

Note 3 to entry: The equivalent wavelength can be calculated from factors related to the instrument design, calibrated experimentally, or determined as part of the CSI signal analysis (see Clause A.3).

3.13
width of the modulation envelope
scan length over which the signal strength represented by the *modulation envelope* (3.10) is greater than a defined value

Note 1 to entry: The width of the modulation envelope is quantifiable in different ways, such as the full width at half maximum (FWHM).

Note 2 to entry: The width of the modulation envelope is related to the coherence length described in ISO 11145:2018, 3.11.4, and is a function of the light source bandwidth (see ISO 25178-600:2019, 3.3.2), the camera spectral sensitivity and geometrical factors such as the numerical aperture of the illumination (see ISO 10934:2020, 3.1.10.4 and ISO 25178-600:2019, 3.3.6).

3.14
phase gap
ϕ_G
<coherence scanning interferometry> offset in units of phase at the *equivalent wavelength* (3.12) between the *CSI scan* (3.2) position for the *interference fringe* (3.7) and the maximum value of the *modulation envelope* (3.10) of a *CSI signal* (3.3)

Note 1 to entry: See Figure 1 for an example CSI signal illustrating the phase gap.

Note 2 to entry: The phase gap is a calculated value that depends on the data analysis method.

Note 3 to entry: The phase gap can vary as a function of optical dispersion in the instrument optics as well as sample surface characteristics such as surface films (see ISO 25178-600:2019, 3.4.1), local slope and optically non-uniform materials (see ISO 25178-600:2019, 3.4.6).

3.15
fringe-order error
2π error
<coherence scanning interferometry> error in the identification of the correct 2π phase interval in a topography map that makes use of the *interference phase* (3.8) as part of the *CSI signal processing option* (3.11)

Note 1 to entry: Fringe-order errors are integer multiples of one-half the *equivalent wavelength* (3.12) in height.

Note 2 to entry: Fringe-order errors can lead to artificial steps within the topography map. On smooth, continuous surfaces, these artificial steps can sometimes be corrected by using phase unwrapping algorithms (see ISO/TR 14999-2:2019, 6.6)

4 Instrument requirements

An instrument according to this document shall perform areal surface topography measurements of a sample surface using CSI. The instrument shall comprise an interferometer (see ISO/TR 14999-2) and means to perform a CSI scan. The instrument shall acquire camera images captured at scan positions determined by a CSI scan increment. The data acquisition proceeds at a CSI scanning rate over a CSI scan length. The CSI signal for a single image point shall comprise interference fringes having an interference phase and modulation amplitudes shaped by a modulation envelope characterized by the width of the modulation envelope. The instrument shall convert acquired data to an areal topography using a CSI signal processing option that uses the interference fringes or modulation envelope, or both. The topography height values shall be inferred from either the CSI scanning rate or the equivalent wavelength, or both. If the final surface topography relies on the interference phase, the CSI signal processing option shall take into account the phase gap when interpreting the interference fringes, so as to avoid fringe-order errors.

Figure 2 shows the information flow between these elements for a CSI microscope, from the real surface to a scale-limited surface. Example CSI hardware, techniques and error sources are given in Annexes A and B.

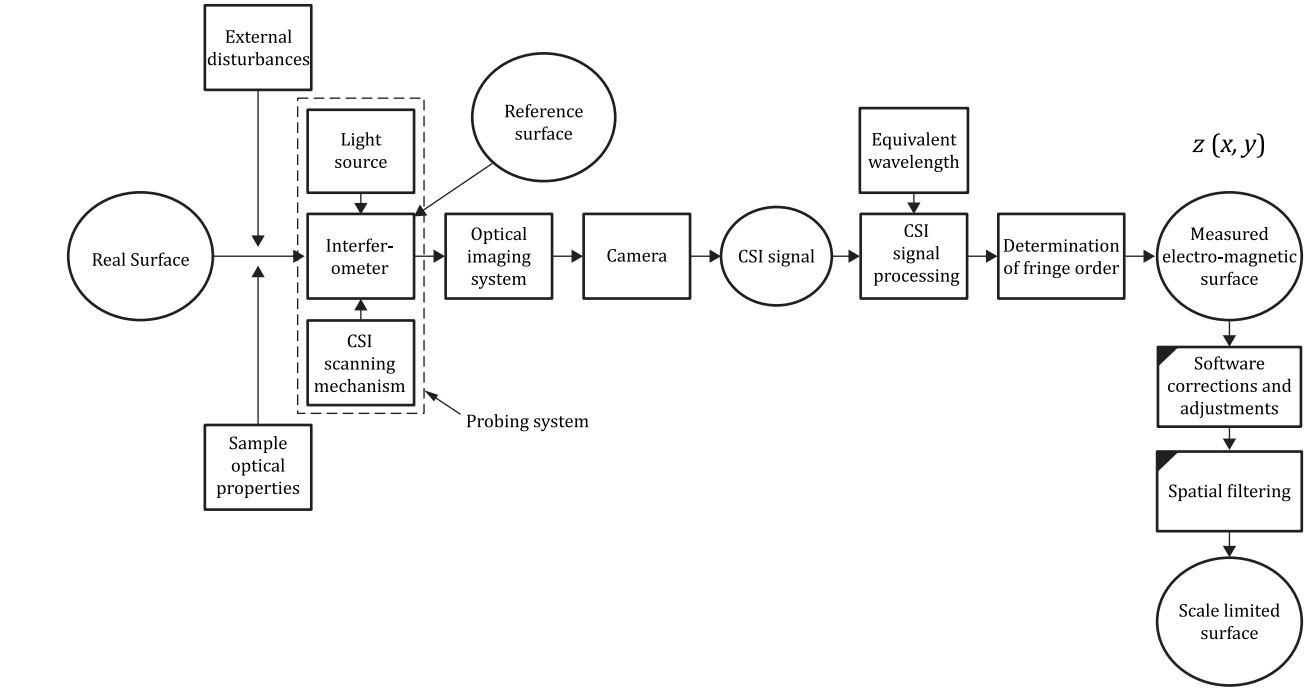

Key

measurand

operator with intended modification

operator without intended modification

Figure 2 — Information flow concept diagram for CSI

5 Metrological characteristics

The standard metrological characteristics for areal surface texture measuring instruments specified in ISO 25178-600 shall be considered when designing and calibrating the instrument.

Annex B describes sources of measurement error that can influence the calibration result.

6 Design features

Standard design features described in ISO 25178-600 shall be considered in the design.

Annex A provides examples of specific design features of CSI instruments.

7 General information

The relationship between this document and the GPS matrix model is given in Annex C.

Annex A
(informative)

Principles of CSI instruments for areal surface topography measurement

A.1 General

CSI is a mature technology and there are substantial resources in existing ISO documents listed in the bibliography and in the published literature regarding instrument design and theory of operation.[25][26][27][28] This annex is a summary with the goal of clarifying terms and definitions as well as some of the influence quantities that contribute to the metrological characteristics of CSI.

A.2 Instrument design

Figure A.1 provides an illustration of an example CSI microscope system based on a Michelson interferometer.[2][16][29][30][31]

The scanning mechanism G imparts a controlled variation of optical path length by means of an axial scan of the sample part along the *z*-axis direction (see ISO 25178-607:2019, 3.5). The sample surface lies nominally within the plane, consistent with the coordinate system defined in ISO 25178-600:2019, 3.1.2, and is imaged to the electronic camera. Superimposed onto the image of the sample is an interference pattern or interferogram resulting from the coherent superposition of the light from the sample surface and from the reference surface (see ISO/TR 14999-2:2019, 6.2.1).

CSI instruments configured as microscopes often have interchangeable interference objectives (see ISO 25178-603) in place of conventional microscope objectives (see ISO 10934:2020, 3.1.106). These objectives have built-in beam splitters and reference surfaces.[25][26][27][32][33][34][35] CSI microscopes can have the scanning mechanism as part of the part support or integrated into the mount for the interference objective.

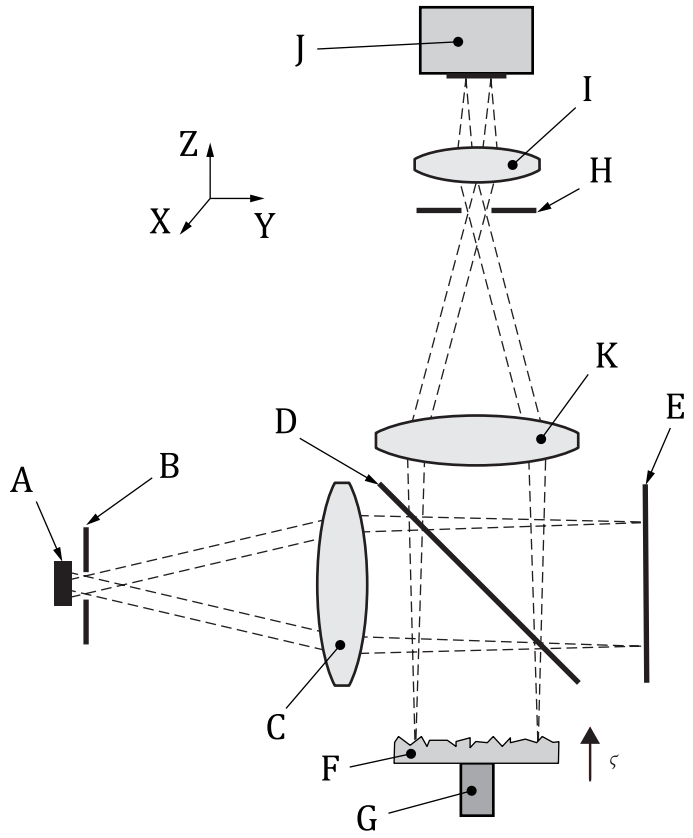

Key

A	light source	F	workpiece
B	illumination aperture stop	G	scanning mechanism
C	condensing lens	H	imaging aperture stop
D	beamsplitter	I	camera lens
E	reference mirror	J	camera
ζ	scanning motion	K	tube lens

Figure A.1 — Schematic diagram of a Michelson-type CSI microscope

The measurement principle is to determine the surface height at each point on the sample surface by analysis of multiple interference patterns recorded as CSI signals for each image point acquired during a sequence of controlled CSI scan positions. Figure A.2 shows the camera image at different scan positions during a data acquisition scan, illustrating the changes in the appearance of the fringes that correspond to horizontal slices through the object surface topography. Note that elements related to the camera and imaging system that were shown in Figure A.1 are also part of the assembly but are not shown in Figure A.2.

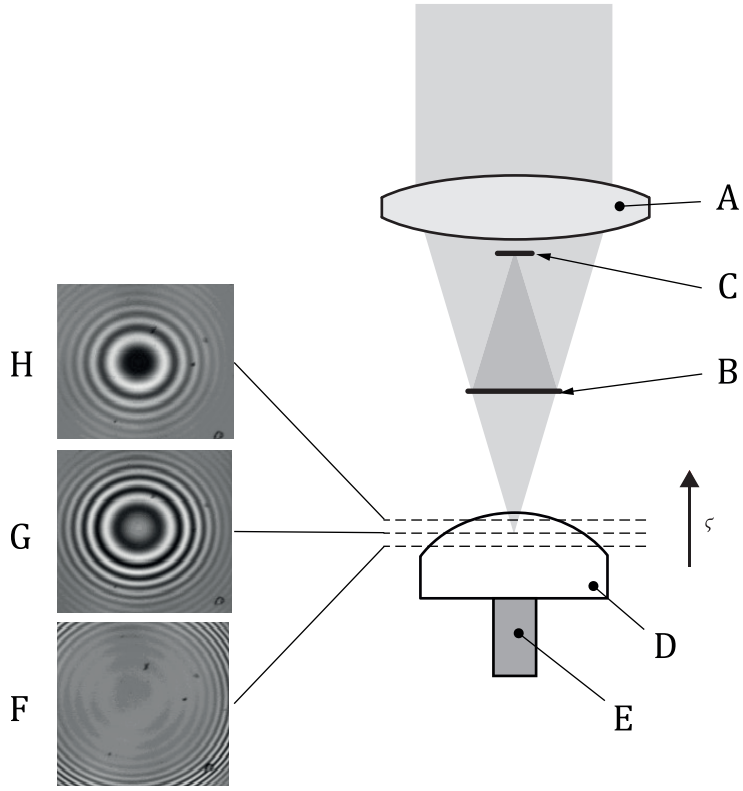

Key

A	objective lens	E	scanning mechanism
B	interferometer beamsplitter	F	image at beginning of the scan
C	reference mirror	G	image at midpoint of the scan
D	workpiece	H	image at end of the scan
ζ	scanning motion		

NOTE Figure A.2 shows a conceptual drawing of data acquisition for a CSI microscope equipped with a Mirau-type interference objective lens.

Figure A.2 — Conceptual drawing of data acquisition for a CSI microscope

A characteristic of most CSI systems is that the reported areal surface topography is everywhere in focus, even if the topography variations are much greater than the depth of field of the objective lens. This characteristic assumes that the objectives are adjusted such that the position of best focus and the peak of the modulation envelope are coincident.[32] For microscope systems that scan the interference objective, the objective lenses are of the infinite conjugate type, meaning that a point on the object is imaged at infinity (see ISO 9335:2012, 4.4.2.3, and ISO/TR 14999-1:2005, 4.1).

Light sources for CSI are most commonly spatially incoherent and spectrally broadband or white light, exemplified by incandescent lamps or white-light or broadband light-emitting diodes (see ISO 10934:2020, 3.1.73). CSI instruments are also realized with light sources in the blue, green, red or infrared wavelengths. The light source can include interchangeable filters for adjusting the illumination spectrum (see ISO 10934:2020, 3.1.38.7). For dynamically moving objects, such as oscillating microstructures, the light source can be flashed at high speed to stroboscopically freeze the object motion.[37][38][39]

For a CSI microscope, the light source is often imaged into the objective pupil in the epi-illumination Köhler geometry (see ISO 10934:2020, 3.1.73.2 and 3.1.73.3). Many instruments have adjustable light stops for controlling the size of the illumination field as well as the illumination aperture (see ISO 10934:2020, 3.1.10.4).[25] In Figure A.1, an illumination aperture stop B controls the numerical aperture (NA) of the illumination, while an imaging aperture stop H controls the imaging NA.

Depending on the measurement task, it can be useful to have a small diameter aperture stop (component B in Figure A.1), or equivalently, a small light source, such that the CSI instrument illuminates the sample with an almost parallel beam. A small illumination NA facilitates a large working distance, shadowing is avoided and deep surface features can be investigated. However, a small illumination NA reduces the lateral resolution compared to completely filling the entrance pupil of the objective.

Cameras for the visible wavelengths can be of the charge-coupled device (CCD) or complementary metal-oxide semiconductor (CMOS type), with a format ranging from 300 000 pixels to over 4 million pixels. The sampling interval as described in ISO 25178-600:2019, 3.1.17 is determined by the camera format and the optical magnification (see Clause B.10).

The topographic lateral resolution defined in ISO 25178-600 summarizes the net effect of the camera, optics and data processing on the ability of the instrument to resolve closely spaced topographical features on the surface (see also Clauses B.9 and B.10). The net effect of the camera, optics and data processing on the topographic lateral resolution can be determined in accordance with ISO 25178-700. For example, the instrument transfer function (ITF) defined in ISO 25178-600:2019, 3.1.19 as a curve, describes an instrument's height response as a function of the spatial frequency of the surface topography. Another approach is given by using the topography fidelity, defined in ISO 25178-600:2019, 3.1.26. The lateral resolution and the ITF can vary with specific surfaces structures comprising steep slopes, sharp edges or high aspect ratios. Further information on the ITF can be found in References [2], [40], [41] and [42].

Adjustments upwards or downwards of the position of the objective or a sample stage (not shown in Figure A.1) brings the test surface into focus (see ISO 10934:2020, 3.1.65). Part setup can require a nominal adjustment of both focus and tip and tilt, although automation can complete some or all these steps (for example, see "autofocus" as defined in ISO 10934:2020, 3.2.4).

The CSI scan length is often between 10 µm and 400 µm for piezoelectric scanners. For motorized scanners, the scan length can be 70 mm or more.[31] In that CSI measures surface heights by referencing to CSI scan position, knowledge of the scanner position is important to the overall accuracy of the CSI instrument.[25] Although less common, it is feasible to move the reference mirror, beam splitter or some other combination of optical elements to perform a CSI scan. With a moving reference mirror, the depth of field determines the range of surface heights accommodated by the instrument.

A.3 CSI theory of operation

As illustrated in Figure 1, a CSI signal is characterized by oscillating interference fringes and an overall modulation envelope. Depending on the data analysis mode and the instrument design, surface topography measurements are based on the location of the modulation envelope at each image point during the CSI scan or the interference phase, or both.

An approximate mathematical model of a CSI signal $I(x,y)$ is shown in Formula (A.1):

$$I(x,y)=I_{\mathrm{DC}}(x,y)+I_{\mathrm{AC}}(x,y)\,\exp\left[-(z(x,y)-\zeta)^2/2\sigma^2\right]\cos\left[\frac{4\pi(z(x,y)-\zeta)}{\lambda_{\mathrm{eq}}}+\phi_{\mathrm{G}}\right] \tag{A.1}$$

where

$I_{\mathrm{DC}}(x,y)$ is the background intensity;

$I_{\mathrm{AC}}(x,y)$ is the interference fringe intensity;

$z(x,y)$ surface height for an individual image point;

ζ is the scan position.

In systems with low illumination and NA (see ISO 10934:2020, 3.1.10.4, and ISO 25178-607), the equivalent wavelength λ_{eq} is close to the mean spectral emission wavelength of the light source. The phase gap ϕ_{G} is the distance expressed in terms of interference phase between the modulation peak position and the central bright fringe of the interference pattern. The standard deviation σ is for a Gaussian modelling of the

modulation envelope. The width and shape of the modulation envelope relates to spectral and geometric factors that limit both the temporal and spatial coherence.[19] More exact models of CSI signals have a more complicated form.[43]

The general strategy for data analysis is to measure the surface topography by identifying a feature of the modulation envelope, such as the peak, the centroid or the position of stationary phase. As an example, in Formula (A.1), the maximum value of the modulation envelope is for $z = \zeta$; therefore, the scan position for which the modulation envelope reaches its peak value is a measure of surface height. A topography measurement using the modulation envelope is sometimes referred to as the "coherence profile" or "coherence map",[44] and can be the final reported areal surface topography for optically rough surfaces (see ISO 25178-600:2019, 3.4.5).

A common signal processing option is to refine the topography by analysis of the interference fringes, e.g. using zero crossings, sinusoidal fitting or the equivalent of phase shifting interferometry (see ISO 25178-603) using data collected near the modulation envelope peak. The initial surface topography measurement using the coherence information determines the appropriate 2π interval for the phase evaluation. A measurement using interference phase is often considered to be more precise or as having a lower measurement noise than the coherence map, but is typically restricted to optically smooth surfaces (see ISO 25178-600:2019, 3.4.4).

A wide range of data acquisition strategies and data processing methods are employed in modern instruments to make use of the modulation envelope alone or together with the interference fringes in the CSI signal described by Formula (A.1). These acquisition strategies and algorithms include electronic envelope detection,[45][46] correlation of the experimental CSI signal with a theoretical or calibrated complex kernel,[47] and Fourier analysis of the frequency content of the CSI signal.[44][48] Summary details of algorithms and data processing methods are provided in References [25], [26], [27] and [28].

A.4 CSI for transparent films profiling

CSI has the ability to separate multiple reflections from semi-transparent film structures on surfaces so as to measure the surface topography over and under these films.[15][49] From Figure A.3, it is apparent that for a single-layer film (see ISO 25178-600:2019, 3.4.3) that is thicker than the width of the modulation envelope, there are two clearly identifiable modulation envelopes corresponding to surface reflections from the film boundaries. An approach to generating surface topography maps over films is to identify the right-most signal as the top-surface signal, as shown in Figure A.3. If the refracting properties of the film are known, the substrate or other secondary surfaces below the top surface can be mapped for height by analysis of the signals that follow the top-surface signal, yielding additional information such as 3D film thickness. CSI instruments may have an adjustable illumination NA, to optimize the signal strength and improve accuracy when viewing through films.[23][50][51]

The thinnest film for which the two signals shown in Figure A.3 can be considered separable is related to the width of the modulation envelope. This lower limit on film thickness is defined informally as the axial response or axial resolution of the CSI instrument,[52] in analogy with optical coherence tomography,[20] optical microscopy[53] (see ISO 10934:2020, 3.1.128.5) and confocal microscopy (see ISO 25178-607:2019, C.2).

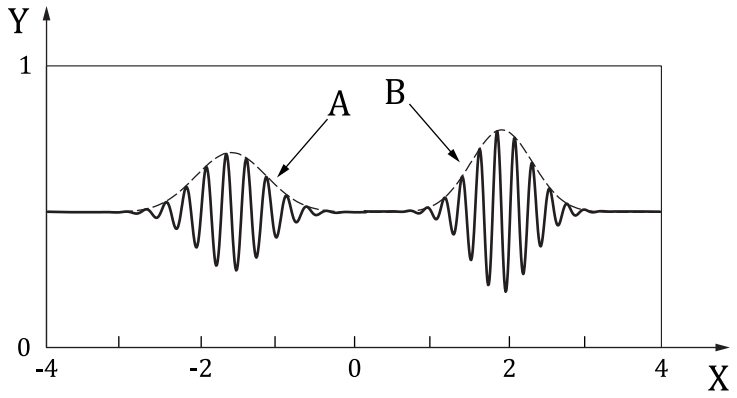

Key

X	CSI scan position, in µm	A	substrate signal
Y	intensity	B	top-surface signal

Figure A.3 — Example CSI signal for a single-layer, partially transparent surface film

A.5 Model-based CSI

Signal modelling allows CSI instruments in many cases to measure surface characteristics beyond the limits of the signal processing methods in Clauses A.3 and A.4.[50] As an example, for thin films (see ISO 25178-600:2019, 3.4.2), the separate signals shown in Figure A.3 can overlap such that it is difficult to clearly separate them. In this case, an approach is to model the expected signal for a range of film thickness. A search through a library of such theoretical signals for a match to an experimental result provides the areal surface topography in the presence of the film, as well as additional dimensional properties of the film layer.[43][55]

The same strategy of modelling the CSI signal can be used to determine areal surface topography in the presence of surface features that are closer together than the topographic spatial resolution (see ISO 25178-600:2019, 3.1.20). Modelling methods include diffraction calculations with variable parameters that include feature height and spacing.[56][57][58][59]

Annex B
(informative)

Sources of measurement error for CSI instruments

B.1 Metrological characteristics and influence quantities

ISO 25178-600:2019, 3.1.28 defines a specific set of metrological characteristics for areal surface topography measuring instruments. These metrological characteristics capture influence quantities, factors that can influence a measurement result and can be propagated through an appropriate measurement model to evaluate measurement uncertainty. See ISO 25178-700 and ISO 12179 for methods for calibration, adjustment and verification of the metrological characteristics.

In this annex, influence quantities are described that affect the metrological characteristics. Knowledge of these influence quantities is not needed for uncertainty analysis if it is feasible to perform a direct calibration of the corresponding metrological characteristics. However, knowledge of influence quantities can be useful for optimizing measurements and minimizing sources of error.

Table B.1 summarizes the influence quantities discussed in this annex.

Table B.1 — Summary of influence quantities and related metrological characteristics

Item	Influence quantity	Relevant metrological characteristic
B.2	Equivalent wavelength	α_z amplification coefficient
B.3	Mean value of the CSI scan increment	α_z amplification coefficient
B.4	Focus effects	T_{FI} topography fidelity W_{R} topographic spatial resolution
B.5	Reference mirror flatness	z_{FLT} flatness deviation
B.6	Optical ray tracing error	z_{FLT} flatness deviation $\Delta x(x,y)$, $\Delta y(x,y)$ *x-y* mapping deviation
B.7	Random environmental vibration	N_{M} measurement noise
B.8	Camera noise	N_{M} measurement noise
B.9	Optical lateral resolution	W_{R} topographic spatial resolution
B.10	Sampling interval	W_{R} topographic spatial resolution
B.11	Optical distortion	$\Delta x(x,y)$, $\Delta y(x,y)$ *x-y* mapping deviation
B.12	Surface films	T_{FI} topography fidelity
B.13	Dissimilar materials	T_{FI} topography fidelity
B.14	Surface slopes and discrete step features	T_{FI} topography fidelity
B.15	CSI scan linearity	l_z linearity deviation
B.16	Fringe-order errors	T_{FI} topography fidelity

B.2 Equivalent wavelength

The use of interference fringe phase to refine the CSI measurement relies on the equivalent wavelength λ_{eq} as the scaling factor for the conversion of phase to surface height. The equivalent wavelength can be calculated from contributions such as the light source wavelength together with other factors related to the instrument design.[60][61] Alternatively, the equivalent wavelength λ_{eq} can be linked directly to the scan increment so that the envelope detection and phase estimation measurements agree in scale.[25][62][63]

The equivalent wavelength is an influence quantity for the amplification coefficient α_z defined in ISO 25178-600:2019, 3.1.10.

B.3 Mean value of the CSI scan increment

In CSI, unlike many other interferometric techniques that rely on the source wavelength to scale the measurement result, the basic unit of measure is the scan increment.[25] The scan increment can be determined by comparison with a material measure such as a step height,[64][65] or by a calibration using the interference effect with a known equivalent wavelength.[66] Some instruments equip the scanner with electronic sensors, such as capacitance sensors, linear variable differential transformers (LVDTs), displacement interferometers, optical encoders or other methods used in feedback systems, to improve scan linearity.[67]

The mean value of the CSI scan increment is an influence quantity for the amplification coefficient α_z defined in ISO 25178-600:2019, 3.1.10.

B.4 Focus effects

In most CSI systems, the position of best focus is coincident with the maximum modulation amplitude. If this is not the case, perhaps because of thermal effects or inadequate adjustment, the interference patterns used to calculate the measured surface topography will be blurred, thereby reducing the modulation amplitude.

Focus effects are influence quantities for the topographic spatial resolution W_R defined in ISO 25178-600:2019, 3.1.20, and the topographic fidelity T_{FI} defined in ISO 25178-600:2019, 3.1.26.

B.5 Reference mirror flatness

For CSI instruments as described in Annex A, the interference pattern is a measure of the difference between the sample surface topography and a reference flat, also referred to as an “areal reference”, as defined in ISO 25178-600:2019, 3.1.1. Therefore, the topography of the reference flat is relevant to accurately measuring surface topography with respect to the areal reference.[68][69]

Reference mirror flatness is an influence quantity for the flatness deviation z_{FLT} defined in ISO 25178-600:2019, 3.1.12.

B.6 Optical ray tracing error

In practice, imperfections in the optical system can have a similar effect to form deviations of the reference flat. These contributions are difficult to distinguish and are often either calibrated or adjusted, or both, at the same time.[70] Optical imperfections can produce flatness deviations that depend on both local slope and the overall orientation of the sample part. Ray tracing errors can be different between an evaluation based on the modulation envelope position and the interference fringe phase and can also depend on the scattering properties of the sample surface.

Optical ray tracing error is an influence quantity for the flatness deviation z_{FLT} defined in ISO 25178-600:2019, 3.1.12 as well as for $x - y$ mapping deviation $\Delta x(x,y)$, $\Delta y(x,y)$ defined in ISO 25178-600:2019, 3.1.13.

B.7 Random environmental vibration

A CSI instrument performs best in an environment isolated from vibration. Often, the instrument is placed on a vibration isolation table, e.g. a rigid slab supported on air-damped legs. The effect of vibration depends strongly on its frequency. Vibrational frequencies well below the camera framerate generate form distortions as a function of sample part orientation, whereas higher frequencies generate cyclic errors that vary from measurement to measurement.[71] The effect of vibrations on specific CSI algorithms and data acquisition methods has been studied in detail.[71][72][73] Some CSI methods can interpret the interference signals to compensate at least in part for the presence of vibration.[74]

Environmental vibration is an influence quantity for the measurement noise N_M defined in ISO 25178-600:2019, 3.1.15.

B.8 Camera noise

In CSI, the imaging camera can be a significant source of random instrument noise (see ISO 25178-600:2019, 3.1.14). The effect of camera noise on the measurement is a function of the data acquisition time, as well as the number of repeat measurements that are used to obtain an average.[71][73][75][76] The effect of camera noise is generally larger when using only the position of the modulation envelope, and improves when including the interference phase information.

Camera noise is an influence quantity for the measurement noise N_M defined in ISO 25178-600:2019, 3.1.15.

B.9 Optical lateral resolution

The lateral resolution depends, among other factors, on the configuration of the lenses, mirrors, light source bandwidth and degree of coherence of the optical system. ISO 25178-600:2019, 3.3 defines optical lateral resolution parameters based on traditional imaging, including the Raleigh criterion, the Sparrow criterion and the Abbe resolution limit, which relate uniquely to the ability of an optical system to clearly separate closely spaced image features in the lateral $x - y$ plane. Lateral resolution can also be specified in terms of the instrument transfer function, which provides the instrument response as a function of lateral spatial frequencies in the topography. See ISO 25178-600:2019, 3.1.19 and References [42], [77], [78] and [79].

Lateral resolution of the optical system is an influence quantity for the topographic spatial resolution W_R defined in ISO 25178-600:2019, 3.1.20.

B.10 Sampling interval

As defined in this document, an electronic camera is a 2D detector array comprised of imaging pixels that map to the sample surface, forming an x-y grid of image points. In object space, i.e. the coordinates of the surface points, the spacing between neighbouring image points is referred to in ISO 25178-600:2019, 3.1.17 as the "sampling interval D_x, D_y", also known as the "lateral sampling interval", "spatial sampling", "lateral sampling" or variants of these terms. An additional factor related to the camera array is the size of the pixels, which map to areas of integration on the sample surface.

The size of the sampling interval depends on the optical magnification and on the physical dimensions of the camera detector array. In a microscope, the sampling interval varies with the selected interference objective and tube lens. If the sampling interval is larger than the optical lateral resolution, then the lateral sampling can be a significant influence quantity in determining the topographic spatial resolution.

Electronic firmware or data processing software can alter the sampling interval, if these system components result in correlation between reported values for neighbouring camera pixels. This can be the case with default noise filtering, or because of a measurement process that includes information from multiple pixels to determine the height of a single image point.

The lateral sampling interval of the optical system is an influence quantity for the topographic spatial resolution W_R defined in ISO 25178-600:2019, 3.1.20.

B.11 Optical distortion

Distortion is an imaging characteristic for an optical system, related both to the approximations inherent in ray tracing through systems far from the optical axis and imperfections in the optical design.[80][81] Common types of distortion include barrel distortion (see ISO 10934:2020, 3.1.4.5.1) and pincushion distortion (see ISO 10934:2020, 3.1.4.5.2).

Optical distortion is an influence quantity for the x-y mapping deviation $\Delta x(x,y)$, $\Delta y(x,y)$ defined in ISO 25178-600:2019, 3.1.13.

B.12 Surface films

A surface film is defined in ISO 25178-600:2019, 3.4.1 as a material deposited onto another surface whose optical properties are different from that surface. Films are common in many applications, either by direct deposition as part of manufacturing, as a temporary consequence of the manufacturing process (e.g. an oil film) or through a natural process such as oxidation.

As noted in Clause A.4, CSI has the ability to distinguish between thick film layers by separation of multiple modulation envelopes. For thinner films, modelling methods can provide the ability to separate film effects from surface heights, as noted in Clause A.5.

The effect of surface films is an influence quantity for the topography fidelity T_{FI} defined in ISO 25178-600:2019, 3.1.26.

B.13 Dissimilar materials

The optical properties of the sample materials can have a significant impact on the measured surface topography for optically non-uniform surface (see ISO 25178-600:2019, 3.4.6). These optical properties affect the shape and position of the modulation envelope as well as phase of the interference fringes.[26] [82][83] These effects can lead to errors in the areal surface topography map related to the phase change on reflection, including artificial steps between the dissimilar materials, and fringe-order error.

The effect of dissimilar materials is an influence quantity for the topography fidelity T_{FI} defined in ISO 25178-600:2019, 3.1.26.

B.14 Surface slopes and discrete step features

The simplified theory of operation described in Clause A.3 for converting interference phase as measured by CSI to surface height is based on a highly simplified model of the instrument with limitations.[80] In particular, the effect of surface slopes that deflect the incident light at an angle through the optical system produces measurement errors that are not quantified using routine calibration methods available for other metrological characteristics.[85] Empirical adjustment of slope-dependent errors is integrated into some instruments, but procedures have not been standardized.[86][87]

An approach to the evaluation of instrument response that includes surface slopes and other problematic surface features is to evaluate instrument response using a theoretical measurement model implemented in software, sometimes known as a “virtual instrument”, and to simulate results over a range of input parameters and operating conditions.[85] Here again, procedures have not been standardized but there are examples of useful models for this purpose.[59][79][88][89][90][91]

The effect of surface slopes and discrete step features is an influence quantity for the topography fidelity T_{FI} defined in ISO 25178-600:2019, 3.1.26.

B.15 CSI scan linearity

As noted in Clause A.3, reported height values are determined from knowledge of the CSI scan increment, which is presumed to be a constant during a nominally linear CSI scan. The linearity of the CSI scanning mechanism is a contributor to the linearity in reported surface height values, and depends on the design of the CSI scanning mechanism. For some scanning instruments, the nonlinearity in the scan cannot be repeatable from measurement to measurement, making it a source of uncertainty that is not easily reduced through compensation or adjustment.

The consistency of the CSI scan linearity is an influence quantity for the linearity deviation l_z defined in ISO 25178-600:2019, 3.1.11.

B.16 Fringe-order errors

The creation of a surface topography map using interference phase information in the CSI signal involves determining the correct 2π phase interval or fringe order for each surface height point. Most often this involves a first estimate of surface topography using information related to the modulation envelope, with assumptions regarding surface characteristics and optical aberrations.[44][92] An alternative to using the phase gap is to apply a phase unwrapping algorithm (see ISO/TR 14999-2:2019, 6.6), which compares phase values between neighbouring image points and removing 2π phase differences between these values.[93]

The effect of fringe-order errors is an influence quantity for the topography fidelity T_{FI} defined in ISO 25178-600:2019, 3.1.26. However, errors in the determination of fringe order are often considered measurement failures rather than statistical factors that can be included in an uncertainty budget.

Annex C
(informative)

Relationship to the GPS matrix model

C.1 General

The ISO GPS matrix model given in ISO 14638 gives an overview of the ISO GPS system of which this document is a part.

The fundamental rules of ISO GPS given in ISO 8015 apply to this document and the default decision rules given in ISO 14253-1 apply to specifications made in accordance with this document unless otherwise indicated.

C.2 Information about this document and its use

This document specifies the methods, specific terminology and exemplary influence quantities for coherence scanning interferometry instruments used to measure profile and areal surface texture.

C.3 Position in the GPS matrix model

This document is a general ISO GPS standard which influences chain link F of the chains of standards on profile and areal surface texture in the GPS matrix model as shown in Table C.1. The rules and principles given in this document apply to all segments of the ISO GPS matrix which are indicated with a filled dot (•).

Table C.1 — Relationship to the ISO GPS matrix model

	Chain links						
	A	B	C	D	E	F	G
	Symbols and indications	Feature requirements	Feature properties	Conformance and non-conformance	Measurement	Measurement equipment	Calibration
Size							
Distance							
Form							
Orientation							
Location							
Run-out							
Profile surface texture						•	
Areal surface texture						•	
Surface imperfections							

C.4 Related International Standards

The related International Standards are those of the chains of standards indicated in Table C.1.

Bibliography

[1] ISO 8015, *Geometrical product specifications (GPS) — Fundamentals — Concepts, principles and rules*

[2] ISO 9335:2012, *Optics and photonics — Optical transfer function — Principles and procedures of measurement*

[3] ISO 10934:2020, *Microscopes — Vocabulary for light microscopy*

[4] ISO 11145:2018, *Optics and photonics — Lasers and laser-related equipment — Vocabulary and symbols*

[5] ISO 14253-1, *Geometrical product specifications (GPS) — Inspection by measurement of workpieces and measuring equipment — Part 1: Decision rules for verifying conformity or nonconformity with specifications*

[6] ISO 14638, *Geometrical product specifications (GPS) — Matrix model*

[7] ISO/TR 14999-1, *Optics and photonics — Interferometric measurement of optical elements and optical systems — Part 1: Terms, definitions and fundamental relationships*

[8] ISO/TR 14999-2:2019, *Optics and photonics — Interferometric measurement of optical elements and optical systems — Part 2: Measurement and evaluation techniques*

[9] ISO 25178-6:2010, *Geometrical product specifications (GPS) — Surface texture: Areal — Part 6: Classification of methods for measuring surface texture*

[10] ISO 25178-603, *Geometrical product specifications (GPS) — Surface texture: Areal — Part 603: Nominal characteristics of non-contact (phase-shifting interferometry) instruments*

[11] ISO 25178-607:2019, *Geometrical product specifications (GPS) — Surface texture: Areal — Part 607: Nominal characteristics of non-contact (confocal microscopy) instruments*

[12] ISO 25178-700, *Geometrical product specifications (GPS) — Surface texture: Areal — Part 700: Calibration, adjustment and verification of areal topography measuring instruments*

[13] R. Windecker, P. Haible, and H. J. Tiziani, "Fast Coherence Scanning Interferometry for Measuring Smooth, Rough and Spherical Surfaces," *Journal of Modern Optics* **42**, 2059-2069 (1995).

[14] M. Davidson, K. Kaufman, and I. Mazor, "The Coherence Probe Microscope," *Solid State Technology* **30**, 57-59 (1987).

[15] B. S. Lee, and T. C. Strand, "Profilometry with a coherence scanning microscope," *Appl Optics* **29**, 3784-8 (1990).

[16] T. Dresel, G. Häusler, and H. Venzke, "Three-dimensional sensing of rough surfaces by coherence radar," *Applied Optics* **31**, 919-925 (1992).

[17] I. Lee-Bennett, "Advances in non-contacting surface metrology", OSA *Technical Digest OTuC1* (2004).

[18] G. S. Kino, and S. S. C. Chim, "Mirau correlation microscope," *Applied Optics* **29**, 3775 (1990).

[19] K. G. Larkin, "Efficient nonlinear algorithm for envelope detection in white light interferometry," *Journal of the Optical Society of America* A **13**, 832 (1996).

[20] J. C. Wyant, "How to extend interferometry for rough-surface tests," *Laser Focus World*, 131-135 (1993).

[21] T. Connolly, "Scanning interferometer characterizes surfaces," *Laser Focus World* **31**, 85-87 (1995).

[22] J. Schmit, and D. Chen. "G*reater Measurement Detail with High-Definition Vertical Scanning Interferometry*," Applications Note AN541 (Veeco Instruments, 2010).

[23] P. de Groot, and X. Colonna de Lega, "Signal modeling for low-coherence height-scanning interference microscopy," *Applied Optics* **43**, 4821 (2004).

[24] A. Dubois, and A. C. Boccara, "Full-Field Optical Coherence Tomography," in *Optical Coherence Tomography*, edited by W. Drexler and J. Fujimoto, chapt.19, pp. 565-591, (Springer Berlin Heidelberg, 2008).

[25] P. de Groot, "Principles of interference microscopy for the measurement of surface topography," *Advances in Optics and Photonics* **7**, 1-65 (2015).

[26] P. de Groot, "Coherence Scanning Interferometry," in *Optical Measurement of Surface Topography*, edited by R. Leach, chapt.9, pp. 187-208, (Springer Verlag, Berlin, 2011).

[27] J. Schmit, "White Light Interferometry," in *Encyclopedia of Modern Optics*, edited by R. D. Guenther, pp. 375-387, (Elsevier, Oxford, 2005).

[28] R. Su, "Coherence scanning interferometry," in *Advances in Optical Surface Texture Metrology*, edited by R. K. Leach, pp. 2.1-2.27, (IOP Publishing, 2020).

[29] P. J. de Groot, X. C. de Lega, and D. A. Grigg, "Step height measurements using a combination of a laser displacement gage and a broadband interferometric surface profiler", *Proc. SPIE* **4778**, 127-130 (2002).

[30] R. Windecker, and H. J. Tiziani, "Optical roughness measurements using extended white-light interferometry," *Optical Engineering* **38**, 1081 (1999).

[31] W. Bauer, "Special Properties of Coherence Scanning Interferometers for large Measurement Volumes," *Journal of Physics: Conference Series* **311**, 012030 (2011).

[32] W. Krug, J. Rienitz, and G. Schulz, *Contributions to Interference Microscopy*, (Hilger & Watts, London, 1964).

[33] V. P. Linnik, "Ein apparat fur mikroskopisch-interferometrische untersuchung reflektierender objekte (mikrointerferometer)," *Doklady Akademiya Nauk S.S.S.R.*, 18–23 (1933).

[34] K. Creath, *Dynamic phase imaging utilizing a 4-dimensional microscope system*, (SPIE, 2011) PWB.

[35] P. J. de Groot, and J. F. Biegen, "Interference microscope objectives for wide-field areal surface topography measurements," *Optical Engineering* **55**, 074110-074110 (2016).

[36] R. Su, M. Thomas, R. K. Leach, and J. Coupland, "Effects of defocus on the transfer function of coherence scanning interferometry," *Optics Letters* **43**, 82-85 (2018).

[37] K. Nakano, H. Yoshida, K. Hane, S. Okuma, and T. Eguchi, "Fringe scanning interferometric imaging of small vibration using pulsed laser diode," *Trans. SICE* **31**, 454-460 (1995).

[38] P. de Groot, "Stroboscopic white-light interference microscopy," *Applied Optics* **45**, 5840 (2006).

[39] E. Novak, and M. Schurig, *Dynamic MEMS measuring interferometric microscope*, (SPIE, 2003) OP.

[40] X. Colonna de Lega, P. de Groot "Lateral resolution and instrument transfer function as criteria for selecting surface metrology instruments", *OSA Proc. Optical Fabrication and Testing OTu1D* (2012).

[41] E. Novak, C. Ai, and J. C. Wyant, "Transfer function characterization of laser Fizeau interferometer for high-spatial-frequency phase measurements", *Proc. SPIE* **3134**, 114-121 (1997).

[42] P. J. de Groot, "The instrument transfer function for optical measurements of surface topography," *Journal of Physics: Photonics* **3**, 024004 (2021).

[43] P. J. de Groot, and X. Colonna de Lega, "Signal modeling for modern interference microscopes", *Proc. SPIE* **5457**, 26-34 (2004).

[44] P. de Groot, X. Colonna de Lega, J. Kramer, and M. Turzhitsky, "Determination of fringe order in white-light interference microscopy," *Applied Optics* **41**, 4571-4578 (2002).

[45] H. Haneishi, "*Signal processing for film thickness measurements by white light interferometry*",Chofu, Tokyo (1984).

[46] P. J. Caber, S. J. Martinek, and R. J. Niemann, "New interferometric profiler for smooth and rough surfaces," in *Laser Dimensional Metrology: Recent Advances for Industrial Application*, Proc. SPIE **2088** pp.195-203 (1993).

[47] P. Sandoz, and M. Jacquot, "Processing of white-light correlograms: simultaneous phase and envelope measurements by wavelet transformation", Proc. SPIE **3098**, (1997).

[48] P. J. de Groot, "Surface profiling by frequency-domain analysis of white-light interferograms", Proc. SPIE **2248**, 101-104 (1994).

[49] M. Davidson, K. Kaufman, I. Mazor, and F. Cohen, "*An Application Of Interference Microscopy To Integrated Circuit Inspection And Metrology*", **0775**, (1987).

[50] P. de Groot, X. Colonna de Lega, D. Grigg "*High-NA interference microscopy of complex surface structures*", Proc. ASPE (2003).

[51] Zygo Corporation, *MetroPro Film Analysis*, Applications Note AN-0001 (2008).

[52] P. de Groot, "The Meaning and Measure of Vertical Resolution in Optical Surface Topography Measurement," *Applied Sciences* **7**, 54 (2017).

[53] M. Srinivasarao, "5 - Recent Advances in Optical Microscopy and its Application to the Characterization of Polymers," in *Comprehensive Polymer Science and Supplements*, edited by G. Allen and J. C. Bevington, pp. 163-196, (Pergamon, Amsterdam, 1989).

[54] X. Colonna de Lega, "Model-Based Optical Metrology," in *Optical Imaging and Metrology*, edited by W. Osten and N. Reingand, chapt.13, pp. 283-304, (Wiley-VCH Verlag, Weinheim, 2012).

[55] M. F. Fay, and T. Dresel, "Applications of model-based transparent surface films analysis using coherence-scanning interferometry," *Optical Engineering* **56**, 111709.1-6 (2017).

[56] P. de Groot, X. Colonna de Lega, J. Liesener, and M. Darwin, "Metrology of optically-unresolved features using interferometric surface profiling and RCWA modeling," *Optics Express* **16**, 3970 (2008).

[57] X. Colonna de Lega, P. de Groot "Optical Topography Measurement of Patterned Wafers", *Proc. ULSI Technology* **CP 788**, 432-436 (2005).

[58] M. Thomas, R. Su, N. Nikolaev, J. Coupland, and R. K. Leach, "Modeling of interference microscopy beyond the linear regime," *Optical Engineering* **59**, 034110 (2020).

[59] J. Coupland, and N. Nikolaev, "Surface scattering and the 3D transfer characteristics of optical profilers", (SPIE, 2020).

[60] G. Schulz, and K.-E. Elssner, "Errors in phase-measurement interferometry with high numerical apertures," *Applied Optics* **30**, 4500 (1991).

[61] J. F. Biegen, "Calibration requirements for Mirau and Linnik microscope interferometers," *Applied Optics* **28**, 1972 (1989).

[62] J. Schmit, M. Krell, and E. Novak, "Calibration of high-speed optical profiler," in *Optical Manufacturing and Testing V*, **5180** pp.355-364 (2003).

[63] P. de Groot "Method and apparatus for surface topography measurement by spatial-frequency analysis of interferograms," US Patent 5,398,113 (1995).

[64] VDI/VDE 2655, *Part 1.3: Calibration of interferometers and interference microscopes for form measurement (Verein Deutscher Ingenieure/Verband der Elektrotechnik, Elektronik und Informationstechnik, Beuth-Verlag, 2020).*

[65] P. de Groot, and D. Fitzgerald, "Measurement, certification and use of step-height calibration specimens in optical metrology", Proc. SPIE **10329**, 1032919.1-1032919.9 (2017).

[66] P. de Groot, and J. Beverage, "Calibration of the amplification coefficient in interference microscopy by means of a wavelength standard", Proc. SPIE **9526**, 952610-952610-11 (2015).

[67] A. Olszak, and J. Schmit, "High-stability white-light interferometry with reference signal for real-time correction of scanning errors," *Optical Engineering* **42**, 54-59 (2003).

[68] K. Creath, and J. C. Wyant, "Absolute measurement of surface roughness," *Applied Optics* **29**, 3823 (1990).

[69] C. L. Giusca, R. K. Leach, F. Helary, T. Gutauskas, and L. Nimishakavi, "Calibration of the scales of areal surface topography-measuring instruments: part 1. Measurement noise and residual flatness," *Measurement Science and Technology* **23**, 035008 (2012).

[70] C. Hovis, H. Shahinian, C. Evans "Observations on the effect of retrace error in scanning white light interferometry of smooth optical surfaces", Proc. OFT OM4A.2 (2019).

[71] P. J. de Groot, "Interference Microscopy for Surface Structure Analysis," in *Handbook of Optical Metrology*, edited by T. Yoshizawa, chapt.31, pp. 791-828, (CRC Press, 2015).

[72] P. J. de Groot, "Vibration in phase-shifting interferometry," Journal of the Optical Society of America A **12**, 354-365 (1995).

[73] P. de Groot, "Design of error-compensating algorithms for sinusoidal phase shifting interferometry," *Applied Optics* **48**, 6788 (2009).

[74] J. R. Troutman, C. J. Evans, and T. L. Schmitz, "Vibration effects on an environmentally tolerant scanning white light interferometer", *Proc. American Society for Precision Engineering* **59**, 47-50 (2014).

[75] C. P. Brophy, "Effect of intensity error correlation on the computed phase of phase-shifting interferometry," *Journal of the Optical Society of America* A **7**, 537 (1990).

[76] P. de Groot, and J. DiSciacca, "Surface-height measurement noise in interference microscopy", Proc. SPIE **10749**, 107490Q-1 - 107490Q-9 (2018).

[77] P. de Groot, X. Colonna de Lega "Interpreting interferometric height measurements using the instrument transfer function", Proc. FRINGE 30-37 (2006).

[78] E. Church, and P. Takacs, "Effects Of The Optical Transfer Function In Surface Profile Measurements", Proc. SPIE **1164**, 2-15 (1989).

[79] R. Su, J. M. Coupland, C. J. R. Sheppard, and R. K. Leach, "Scattering and three-dimensional imaging in surface-topography measuring interference microscopy," *Journal of the Optical Society of America* A **38**, 27-42 (2020).

[80] W. J. Smith, *Modern Optical Engineering*, (SPIE Press, Bellingham, WA, 2007).

[81] P. Ekberg, R. Su, and R. Leach, "High-precision lateral distortion measurement and correction in coherence scanning interferometry using an arbitrary surface," *Optics Express* **25**, 18703-18712 (2017).

[82] A. Harasaki, J. Schmit, and J. C. Wyant, "Offset of Coherent Envelope Position Due to Phase Change on Reflection," *Applied Optics* **40**, 2102 (2001).

[83] T. Doi, K. Toyoda, and Y. Tanimura, "Effects of phase changes on reflection and their wavelength dependence in optical profilometry," Applied Optics **36**, 7157-7161 (1997).

[84] P. de Groot, X. Colonna de Lega, R. Su, and R. K. Leach, "Does interferometry work? A critical look at the foundations of interferometric surface topography measurement", Proc. SPIE **11102**, 111020G.1 - 111020G-11 (2019).

[85] R.K. Leach, P.J. de Groot, H. Haitjema "Infidelity and the calibration of surface topography measuring instruments", Proc. ASPE 1-7 (2018).

[86] L. L. Deck, and C. Evans, "High performance Fizeau and scanning white-light interferometers for mid-spatial frequency optical testing of free-form optics", Proc. SPIE **5921**, 59210A-59210A-8 (2005).

[87] X. Colonna de Lega, T. Dresel, J. Liesener, M. Fay, N. Gilfoy, K. Delldonna et al. “Optical form and relational metrology of aspheric micro optics”, Proc. ASPE **67**, 20-23 (2017).

[88] P. de Groot, and X. Colonna de Lega, “Fourier optics modelling of interference microscopes,” J. Opt. Soc. Am. A **37**, B1-B10 (2020).

[89] R. K. Leach, C. Giusca, H. Haitjema, C. Evans, and X. Jiang, “Calibration and verificat*ion of areal surface texture measuring instruments”,* CIRP Annals - Manufacturing Technology **64**, 797-813 (2015).

[90] Y. Zhou, J. Troutman, C. J. Evans, and A. D. Davies, “Using the random ball test to calibrate slope dependent errors in optical profilometry”, *OSA Technical Digest* (online) OW4B.2 (2014).

[91] R. Su, and R. K. Leach, “Physics-based virtual coherence scanning interferometer for surface measurement,” *Light: Advanced Manufacturing* **2**, 1 (2021).

[92] A. Harasaki, J. Schmit, and J. C. Wyant, “Improved vertical-scanning interferometry,” *Applied Optics* **39**, 2107-2115 (2000).

[93] D. C. Ghiglia, and M. D. Pritt, *Two-Dimensional Phase Unwrapping, Theory, Algorithms, and Software*, (John Wiley & Sons, New York, 1998).

[94] ISO 12179, *Geometrical product specifications (GPS) — Surface texture: Profile method — Calibration of contact (stylus) instruments*

ICS 17.040.20
Price based on 23 pages